

CRACK PROPAGATION MECHANISM STUDY ON BISMUTH CONTAINED SN BASE LEAD FREE SOLDER UNDER THERMO-MECHANICAL STRESS

Imbok Lee and Young-Woo Lee
MK Electron Co., Ltd., Sejong University
Seoul, Korea
iblee@mke.co.kr; ywlee@mke.co.kr

Aakash Valliappan and Tae-Kyu Lee, Ph.D.
Portland State University
OR, USA
tklee@pdx.edu

ABSTRACT

The needs of the higher thermo-mechanical reliability performance in the Tin-based lead-free solder interconnections are drastically increased in wafer-level chip scale packages implemented in automotive field application. This study reveals that a few wt% Bismuth makes 64% improvement in thermo-mechanical reliability results compared with SAC405 solder. In this study, 12mm X 12mm X 1mm thickness 228LD CTBGA package assembled on 62mil thickness board with NSMD Cu-OSP pad using a SAC305 solder paste. This study is aimed to verify the key mechanism, which enabled the reliability improvements. The crack propagation path shifted with Bismuth contents variation in the lead-free solder interconnections under thermal cycling with -40 to 125°C temperature range and 10°C ramp rate. Microstructure has been studied via polarized optical imaging and High-speed EBSD (electron backscattering diffraction) analysis. The associated grain structure evolution was observed, revealing identifiable signature grain structure development during thermal cycling. Along with the microstructure evolution during thermal cycling, detail resistance monitoring for each localized daisy chain enabled the comparison between various solder materials showing the crack initiation and propagation phenomenon. With this analysis, the decoupling of crack initiation and propagation was performed.

Key words: Thermal cycling reliability, Bismuth, Lead-free solder, Crack propagation mechanism

INTRODUCTION

Since Bismuth-containing Tin based lead-free solder has been introduced¹, it has attracted attention due to its high strength and reliability performance compared to general SAC-based lead-free solder². In the several investigations in the past^{1,3,4,5,6}, bismuth added Tin-based lead-free solder has higher tensile strength, higher yield strength, and lower elongation than normal SAC solders. Because

Bismuth has a role of the precipitation hardening and the suppressing the growth of Ag₃Sn on the solder bulk. But large amount of Bismuth in the solder makes weaker solder joint due to the segregation near the interfacial IMCs⁷.

Recently, it gained attention again^{3,8,9,10} because of demand on higher performance need than conventional SAC solder in large die size wafer level package configuration and specific application in automotive sector¹¹. In the large die adopted package, its CTE (coefficient of thermal expansion) mismatch between the package and the board becomes larger, solder joint undergoes severe stress. In this situation, Bismuth-contained solder's strong mechanical strength is helped to endure the external stress effectively. Of course, the Bismuth amount in the solder has to be controlled a certain amount to reduce the segregation effect of the Bismuth in the solder.

In this study, the thermal cycling reliability characteristics of solder containing a small amount of Bismuth which is below 4wt% in accordance with the new requirements were investigated. To verify the effect of the Bismuth in the solder, the crack initiation and propagation in the solder joint according to the Bismuth content were observed by the polarized optical microscope and the high-speed EBSD what can be shown the grain structure change during the thermal cycling test.

EXPERIMENTAL PROCEDURE

For Simulating a large die effect on the package, thin profile fine pitch BGA type 12mm x 12mm x 1mm height CTBGAs with 10.05mm x 10.05mm die was used. Only one BGA ball is out of the die bottom the package. So, except the outer ball row, whole BGA balls affect of the die effect. Figure 1 (a) shows the component configuration and the die position clearly. It has 228 solder interconnects with 0.5 mm pitch and a surface finish of electrolytic Ni/Au pad.

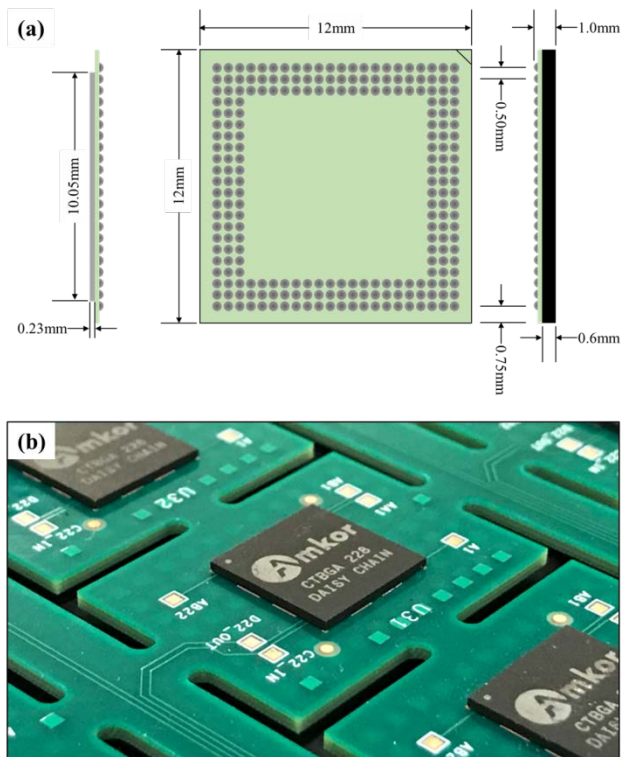


Figure 1. Test vehicle schematics and board level mounted image.

To verify the Bismuth effect, 2.5 wt% silver based 1.0 wt% Bismuth added SAC solder (MXT2) and 4.0 wt% silver based 3.5 wt% Bismuth added SAC solder (MXT4) are selected for this study as likes Table1. For the baseline comparison, 4.0wt% silver based SAC405 was chosen for the reference solder alloy.

Table 1. Tested solder alloy composition

Solder name	Solder alloy composition
SAC405	SAC405
MXT02	SAC2508 with 1.0wt%Bi
MXT06	SAC405 with 3.5wt%Bi

The printed circuit board with a thickness of 1.57 mm on a 6 Cu layer was used for the board level reliability test. This board has a Copper organic surface preservative (Cu-OSP) pad and NSMD pad configuration as shown in Figure 1 (b). Board level mounting was performed using SAC305 Type4 solder paste by using a 100um thickness laser-drilled stencil. to avoid the void effect, whole bumps are inspected by the X-ray. in the X-ray result, whole bumps have less than 25% void in the individual bump. To evaluate the thermal cycling reliability, a thermal cycling test condition G in JEDEC JESD22-A104E is chosen which is -40°C to 125°C thermal cycle with 10°C/minutes ramping rate and 10minute dwell time. To measure the real-time resistance of each unit, a multi-channel data logger and signal extension unit was used. The microstructure of the solder joint is analyzed by polarized optical microscope and is high-speed EBSD.

RESULT AND DISCUSSION

In Figure 2 and Table 2, the thermal cycling test results show a clear indication that Bi contained solder alloys are higher reliability performance based on the thermal cycling test. The initial failures of SAC405, MXT2, and MXT6 are 1284, 1790, and 2124, respectively, and the life expectancy obtained by curve fitting of the Weibull plot is 1881, 2249, and 3078, respectively. In addition, a Beta slope of SAC405 and MXT2 are 11.1847 and 12.3577 respectively, and MXT6 is 8.4891, so that cycle duration from initial failure to final failure also shows that it becomes longer with the content of Bismuth as shown in Figure 3. By simple comparison, the Bismuth amount in the solder has a role of extending its reliability life. compare to the SAC405, MXT2 has 1.4 times and MXT6 has 1.65 times better performance. The beta value of the Weibull parameter estimate - the slope of the Weibull curve - also shows the Bismuth adding makes delayed the failure occurred during the thermal cycling test. Even if, MXT2 has more thermal cycling reliability performance than a normal SAC405, a time takes from an initial failure to a final failure almost similar trend. However, MXT6 is more time takes to the final failure compared to a SAC405 and the MXT2. This reliability result is investigated more deeply by the resistance change during the thermal cycling test.

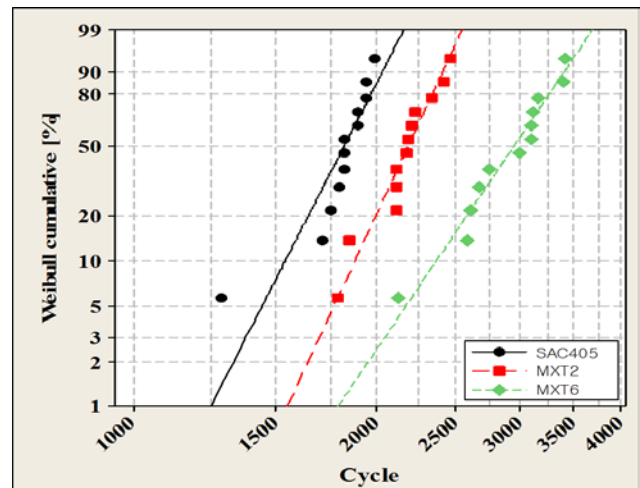


Figure 2. Thermal cycling reliability test result of each solder alloy.

Table 2. Weibull estimates parameters of each solder alloy for the thermal cycling reliability test

Weibull parameter estimates			
	SAC405	MXT2	MXT6
α	1881.76	2249.88	3078.44
β	11.1847	12.3577	8.4891

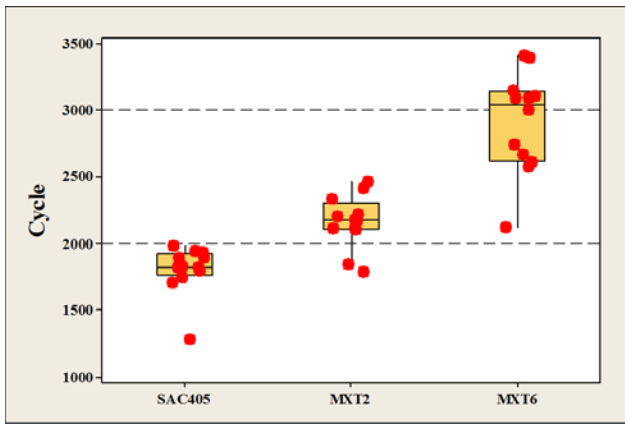


Figure 3. Failure cycle distribution of solder alloy. A Red dot means each components failure cycle point.

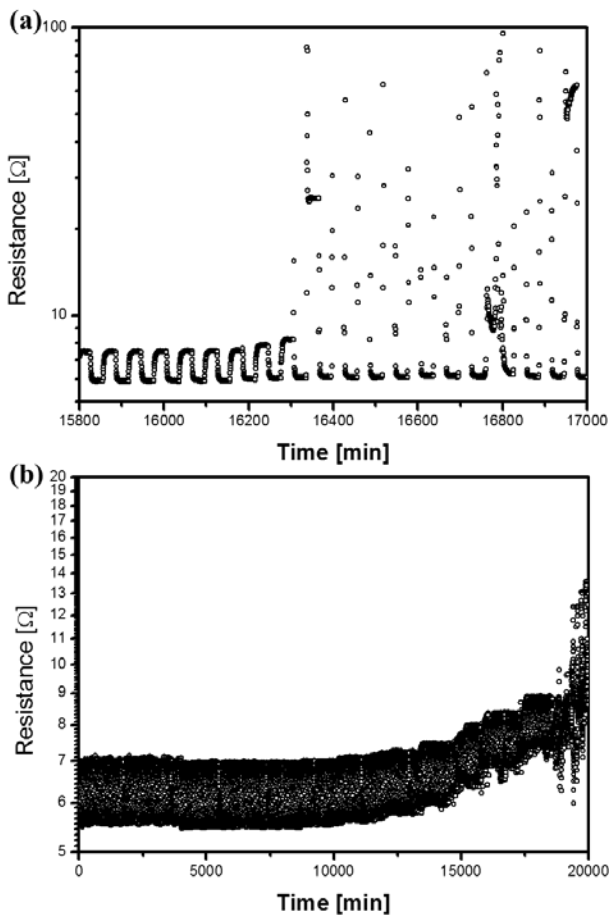


Figure 4. two different resistance trends during the thermal cycling reliability test.

Table 3. The resistance change characteristics of each solder alloy according to the Figure 4

	SAC405	MXT2	MXT6
Category 1	10	5	4
Category 2	2	7	8

The associated thermal cycling result can be confirmed by the resistance change of each unit. The failure criteria were defined as that the change in resistance increases by more than 20% of the initial value. As a result, the resistance change according to the thermal cycling is

segmented into two categories as presented in Figure 4. Category 1 is when the time required to reach the failure criteria is short – approximately within 10 cycle likes Figure 4 (a). Once the resistance change occurs, the resistance change increases every cycle as the thermal cycle increases – cycle to full failure is around 10 cycle. The other category 2, which is presented in Figure 4 (b) – is that the resistance change with the progress of each cycle is gently increased after the first change of resistance occurs, it is seen as a linear curve form on the graph and it takes a long time to reach the failure criteria. Considering this defined failure path and segmenting each thermal cycling component, each component thermal cycling behavior can be listed in Table 3. Category 1 is mainly seen in SAC405, and category 2 is mainly seen in MXT2 and MXT4. This potentially means there is a different degradation mechanism in Bismuth added solder, which delayed the crack propagation rate. As Shown in Figure 5, a total resistance of solder joint is composed by a resistance of interfacial IMC on a component side pad side, a resistance of interfacial IMC on a board side pad, and a resistance of solder bulk. The resistivity of a solder bulk and an interfacial IMC is an order of 10⁻⁶ ohm-cm, whereas a resistivity of a crack is infinite. Thus, after a crack is initiated a resistance of crack path becomes the major resistance change likes Figure 5 (b).

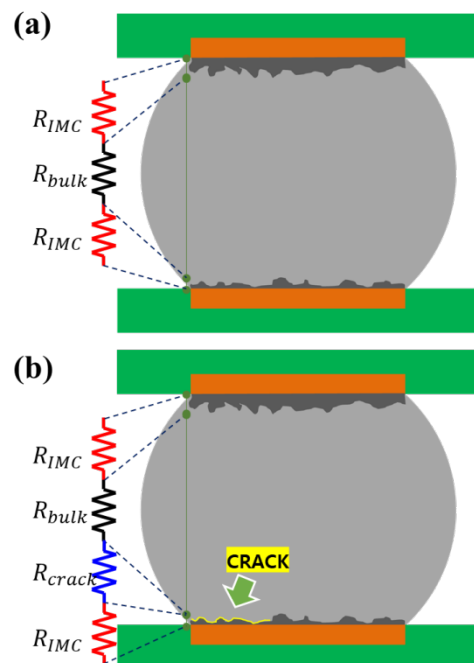


Figure 5. Schematics of a resistance composition on the solder joint. (a) solder joint without crack, and (b) solder joint with a crack occurrence. R_{IMC} (red) is the resistance of an interfacial IMC, R_{bulk} (black) is the resistance of a solder bulk, and R_{crack} (blue) is the resistance of a crack.

After the thermal cycling test, microstructure analysis was performed to confirm the crack pattern and the associated solder microstructure. The optical images in Figure 6 are

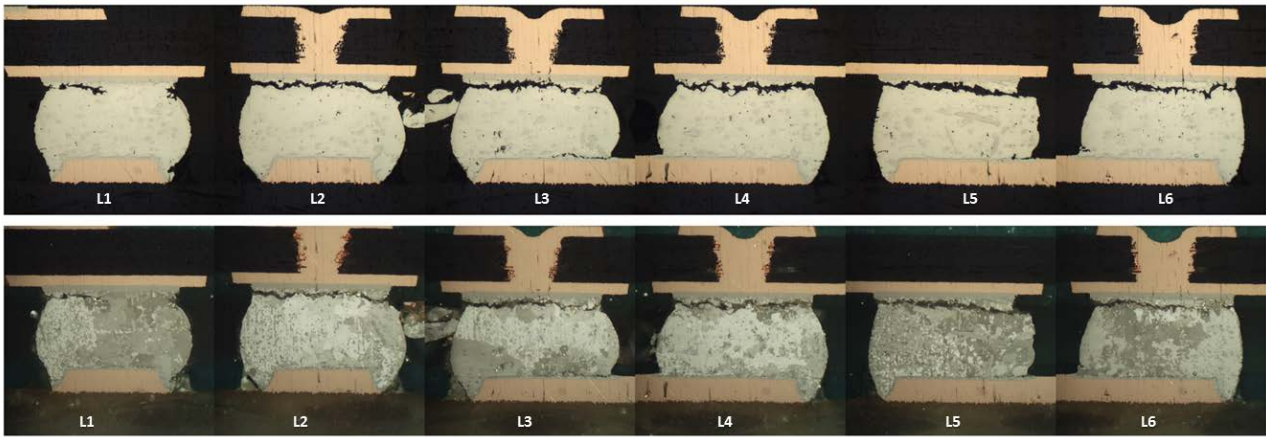


Figure 6. Image of optical microscope and polarized optical microscope of SAC405 solder

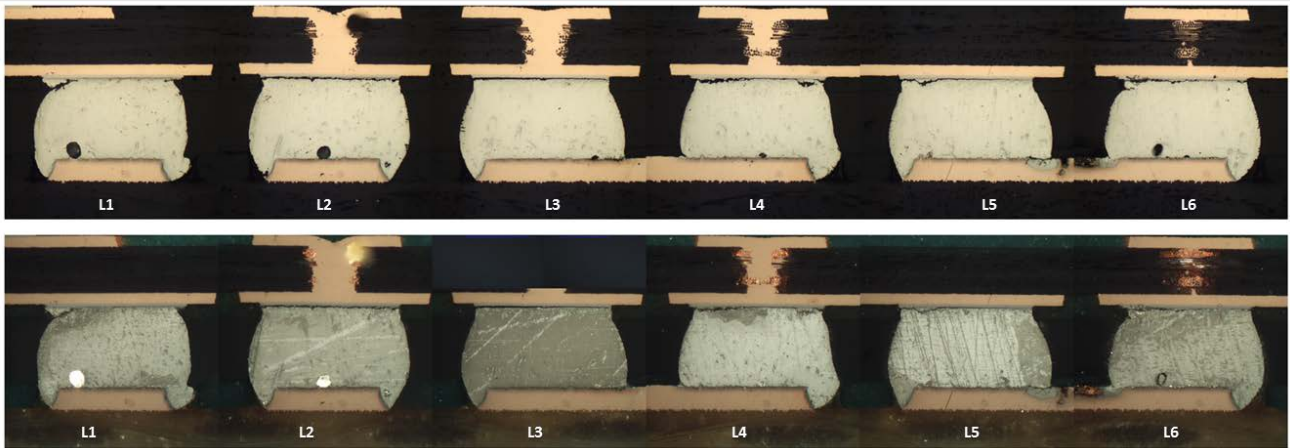


Figure 7. Image of the optical microscope and polarized optical microscope of MXT6 solder.

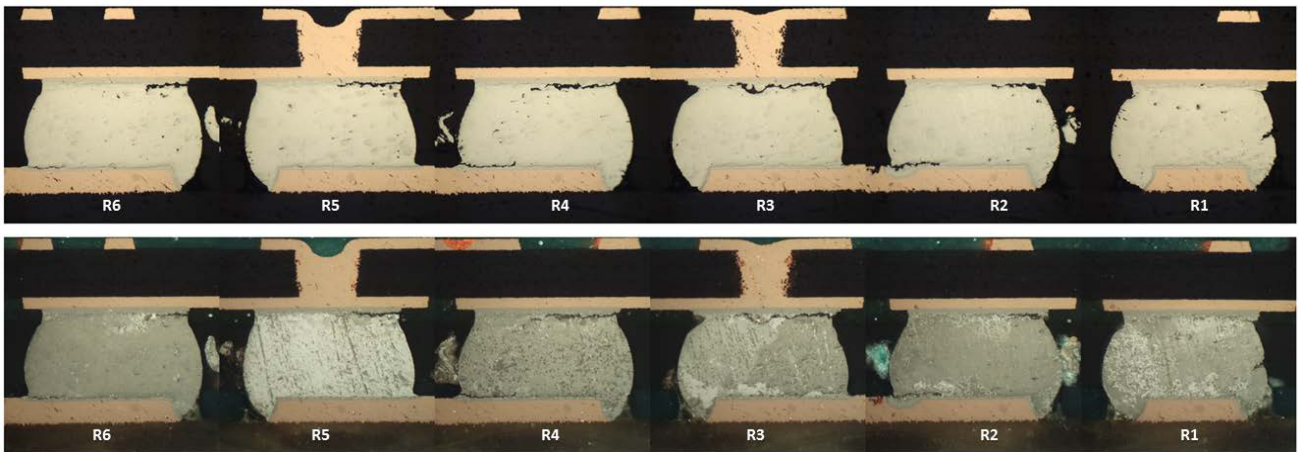


Figure 8. Image of the optical microscope and polarized optical microscope of MXT2 solder

from SAC405, which failed at 1710 cycles. The corner solder joint, the L1 joint shows a partial crack with a full crack in the solder joint, the L2 joint and above. The associated polarized images show a development of recrystallized and refined grain structure near the path of the crack. The grain structure looks normal and aligned with conventional SAC alloy's TC microstructures¹². Compared to 0 to 100 °C temperature ranged thermal cycling tested samples¹³, the refined and Recrystallized grain structures are located more localized and the general region, the which is impacted is less spread in case of -40 to 125 °C temperature ranged thermal cycling condition.

Compared to the SAC405, the optical images in Figure 7 are from MXT6, which failed at 3097 cycles. The corner solder joint, the L1 joint shows a partial crack with a full crack in the L2 joint and above. Unlike the SAC405 sample, the associated polarized images show little to no development of recrystallized and refined grain structure near the path of the crack. The crack propagation is also very close to the interface between the IMC and the solder, which is different from the SAC405 sample joints. The crack propagation in SAC405 occurred near the interface inside the bulk solder, but MXT6 components show a crack path almost at the IMC interface not really

inside the bulk solder. It is clear that the grain refinement and recrystallization are not associated with the crack propagation. A localized grain refinement is observed in the L1 joint, but it did not be transferred into small grain structure. This potentially explains the creep resistance the Bi contained solder is different from the conventional SAC solder alloy, a mechanism, which represents a mitigation of grain boundary sliding¹⁴.

Different signatures were observed in SAC405 and MXT6 samples. The grain refinement and recrystallized grain structure are obvious in SAC405 samples, but MXT6 did not show any recrystallized region near the crack propagation region. The crack in SAC405 samples propagated inside the solder but MXT6 crack propagation occur almost at the IMC interface with little penetration into the solder bulk region. Compared to those two samples, MXT2 shows a grain structure evolution, which is in between the SAC and MXT6 microstructure characteristics. The images in Figure 8 are from MXT2, which failed at 2204 cycles. The R1 joint show a partial crack indicating a higher stress/strain at R2 joint and L2 joint in former cases. The R3 joint is one good representation of the MXT2 behavior. Crack has recrystallized development around the crack region more than MXT6 and less than SAC405. Crack propagation is closer to the IMC interface less close than MXT6 but still

more to the interface than SAC405 solder joint crack propagation paths. But shown in the R6 joint, the crack tip did not cause and developed a large region of recrystallized structures, which is the same phenomenon seen in MXT6 samples. The effect of Bismuth identified in MXT2. Where these results are presenting the same phenomenon as the resistance variation trend in MXT6. Once the crack is initiated, resistance starts to increase, and Bismuth added solder joints have a small increment in the resistance with further thermal cycling. The microstructure development is associated with the grain refinement is also shown in the high-speed EBSD result. As seen in Figure 9, the inverse pole figure (IPF) maps indicate SAC405 has a wide area of subgrain structure development for different orientation that provides a potential region to absorbing and allow further deformation. MXT2 and MXT6 have almost same subgrain orientation, but the uniformity trend of MXT6 is stronger than MXT2. Especially, the cracked localized region in MXT2 shows localized subgrain structure development similar to SAC405. These result show adding Bismuth could control to prevent recrystallization of subgrain, obviously. So, Bismuth added solder has better thermos-mechanical resistance compared with SAC solder.

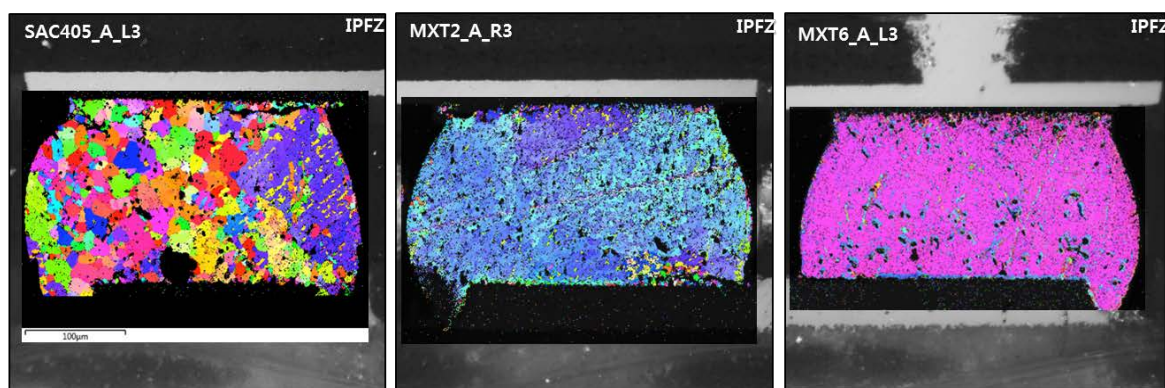


Figure 9. Inverse pole figure maps by high speed EBSD. SAC405 has a wide area of subgrain structure with different orientation. MXT2 and MXT6 have almost same subgrain orientation.

CONCLUSION

The thermal cycling test results identified that Bismuth added solder mitigates recrystallization and grain refinement, which plays a role as a strengthening mechanism and result in thermal cycling reliability performance improvement. It was observed that shift in the crack propagation path from the bulk region to the package side interface, without a subgrain structure development resulted in decreasing the crack propagation rate. Also, it has been observed that the resistance variation, from the initiation to final failure in Bismuth added solder is longer than normal SAC solder.

REFERENCES

- [1] Y. Kariya, M. Otsuka, *Journal of Elec Materi*, V.27, 1998, pp.866.
- [2] F. W. Gayle, G. Becka, A. Syed, J. Badgett, G. Whitten, T. Pan, A. Grusd, B. Bauer, R. Lathrop, J. Slattery, I. Anderson, J. Foley, A. Gickler, D. Napp, J. Mather, C. Olson, *JOM* V.53, 2001, pp.17.
- [3] M. S. Alam, K. R. Hassan, J. C. Suhling, P. Lall, "A Comparative Study of the High Temperature Mechanical Behavior of Lead Free Solders," 2018 17th IEEE Intersociety Conference on Thermal and Thermomechanical Phenomena in Electronic Systems, 2018, pp.1314.
- [4] L. Guo-yuan, S. Xun-qing, *Transactions of Nonferrous Metals Society of China*, V.16, 2006, pp.739.
- [5] Z. Xia, Y. Shi, Z. Chen, *J. of Materi Eng and Perform*, V.11, 2002, pp.107.
- [6] J. Zhao, L. Qi, X. Wang, L. Wang, *J ALLOY COMPD*, V. 75, 2004, pp.196.
- [7] P. Liu, J. Shang, *SCRIPTA MATER*, V.44, 2001, pp.1019.
- [8] P. H. Tsao, T. M. Lu, T. M. Chen, K. C. Chang, C. M. Kuo, M. J. Lii, L. H. Chu, "Board Level Reliability Enhancement of WLCSP with Large Chip Size," 2018 IEEE 68th Electronic Components and Technology Conference, 2018, pp.1200.
- [9] T. Yeung, H. Sze, K. Tan, J. Sandhu, C. Neo and E. Law, "Material characterization of a novel lead-free solder material — SACQ," 2014 IEEE 64th Electronic Components and Technology Conference, 2014, pp.518.
- [10] R. Pandher, R. Healey, "Reliability of Pb-free solder alloys in demanding BGA and CSP applications," 2008 58th Electronic Components and Technology Conference, 2008, pp.2018.
- [11] R. W. Johnson, J. L. Evans, P. Jacobsen, J. R. Thompson and M. Christopher, *IEEE Transactions on Electronics Packaging Manufacturing*, V.27, 2004, pp.164
- [12] T.R. Bieler, B. Zhou, L. Blair, A. Zamiri, P. Darbandi, F. Pourboghra, T. Lee, *Journal of Elec Materi*, V.41, 2012, pp.283
- [13] T. Lee, K. Liu, T. Bieler, *Journal of Elec Materi*, V.38, 2009, pp.2685
- [14] B. Zhou, T. Bieler, T. Lee, K. Liu, *Journal of Elec Materi*, V.39, 2010, pp.2669